SEMARAK ILMU PUBLISHING

Journal of Advanced Research in Fluid Mechanics and Thermal Sciences

Journal homepage:
https://semarakilmu.com.my/journals/index.php/fluid_mechanics_thermal_sciences/index
ISSN: 2289-7879

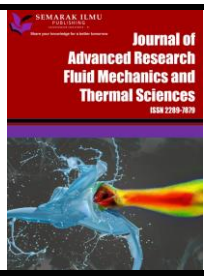

Carboxymethyl Cellulose–Ammonium Formate Biopolymer Electrolyte: Ionic Conductivity and Electrical Properties

Mohd Ibnu Haikal Ahmad Sohaimy[1], Muthiah Muthuvinayagam[2], Mohd Ikmar Nizam Mohamad Isa[1,3,*]

[1] Energy Materials Consortium, Advanced Materials Team, Ionic & Kinetic Materials Research Laboratory (IKMaR), Faculty of Science & Technology, Universiti Sains Islam Malaysia, 71800 Nilai, Negeri Sembilan Darul Khusus, Malaysia
[2] Department of Physics, Saveetha School of Engineering, Saveetha University (SIMATS), Chennai, India
[3] Advanced Nano Materials, Advanced Materials team, Ionic State Analysis (ISA) Laboratory, Faculty of Science & Marine Environment, Universiti Malaysia Terengganu, 21030 Kuala Nerus, Terengganu Darul Iman, Malaysia

ARTICLE INFO

Article history:
Received 16 May 2024
Received in revised form 7 September 2024
Accepted 18 September 2024
Available online 10 October 2024

Keywords:
Solid biopolymer electrolyte; carboxymethyl cellulose; ammonium formate; electrical properties; ionic conductivity

ABSTRACT

Safety concerns about conventional batteries such as prone to leakage, fire and expensive core materials can be overcome by using a solid biopolymer electrolyte (SBE) in the battery system. This work aims to improve the ionic conductivity of the biopolymer electrolyte based on carboxymethyl cellulose (CMC) by doping with varied ammonium formate (AFT) composition (5 – 50 wt.%). The biopolymer electrolyte was tested for its electrical properties, using electrical impedance spectroscopy (EIS) to determine the optimum salt concentration with the highest ionic conductivity. The sample which has the highest ionic conductivity is the sample added with 50 wt.% of ammonium formate which obtained at ~1.47 × 10^{-4} S/cm. Surprisingly, this SBE system shows percolation conductivity behaviour. Within 303K– 373K temperature range, the SBE follow Arrhenius behaviour. The charge carrier's transport properties improved with AFT composition where the dielectric value and relaxation peak position increases with AFT. The maximum ionic conductivity achieved, and the temperature stability shows a promising prospect of current work for energy storage application, albeit further improvement is still needed.

1. Introduction

The continued rise in lithium battery (LIB) consumption has raised serious concern in recent years largely due to the safety issue in operating LIB (leakage and fire) and the sustainability of LIB core materials in the long run since the lithium (Li) minerals are expensive and are one of the rarest metals in earth crust [1,2]. Therefore, current battery technology needs to adopt new approaches to ensure a safer and a feasible future. Finding alternative battery chemistries from materials which are safe, abundant and easily accessible is important.

* *Corresponding author.*
E-mail address: ikmar_isa@usim.edu.my

https://doi.org/10.37934/arfmts.122.1.1930

Solid-state proton conducting electrolyte can improve battery safety by preventing leakage, fire and potentially increase the battery energy density [3]. To fabricate a solid-state electrolyte, polymeric materials such as polyethylene oxide and polyvinyl alcohol can be used to develop a polymer electrolyte (PE). PE has better interfacial for energy storage application compared to the composite electrolyte (CE). The flexibility of PE is also an added benefit as it allows simpler energy storage design and cell stacking [4]. Recently, the use of bio-based polymer (biopolymer) as electrolyte materials has garnered much attention since it possesses similar characteristics/properties as the synthetic polymer but is more environmentally friendly [5]. The preparation method of SBE is also much simpler and not energy intensive. Cellulose based polymer such as carboxymethyl cellulose (CMC) has the capability to be an electrolyte material as shown in previous reports [6-8]. However, CMC SBE has lower ionic conductivity ($<10^{-7}$ S/cm) for any practical application. The low ionic conductivity is due to lack of free charge carriers to facilitate conduction process. Therefore, the charge carrier properties needed to be improved to increase the ionic conductivity of the CMC where this can be done by doping with ionic salts.

Sodium ion (Na^+) and potassium ion (K^+) were mooted as the ideal alternatives to current technology battery (Li^+) since they are both metal-based and exhibits similarity in terms of charge and the energy storage working principle. On top of that, Na^+ and K^+ have several other advantages compared to lithium such as abundance, low-cost, non-toxic and accessible [9,10]. However, Na^+ and K^+ ions are larger than lithium (Li^+). The large ionic size is detrimental in energy storage application as it causes slow diffusion kinetics in the electrode, substantial volume expansion during ions insertion and causing structural collapse (crack) of the electrode. Cracking of the electrode will cause bad grain to grain connections or detachment which leads to poor electrical conductivity, loss of active materials and reduction of battery capacity [11]. Hydrogen or proton (H^+) on the other hand, is an interesting element as it is non-metal and abundant in nature. It is also the smallest and lightest element on earth which makes it a promising charge carrier in energy storage as the small size and mass is favorable in ion transport across the electrolyte and energy storage electrode [12]. Acids and ammonium salts are two types of materials that can supply H^+ for conduction process though acid suffer from chemical breakdown [13]. Ammonium salts are easy to handle and have good solubility in many solvents thus were chosen for this research.

This research focused on improving the ionic conductivity of the CMC based biopolymer electrolyte (SBE) by doping with ammonium salt (ammonium formate, AFT) as H^+ source. The CMC was studied for its ionic conductivity behaviour with different composition of ammonium salt and also at higher temperature. The dielectric behaviour was also investigated to understand the ionic behaviour of the SBE.

2. Methodology

2.1 SBE Preparation

Solution casting method was used to form the CMC-AFT SBE. One gram of CMC was dissolved in 50ml of distilled water by stirring using magnetic stirrer at room temperature. Once dissolved, different compositions of ammonium formate (AFT) salt (5 wt.% - 50 wt.%) was added into the CMC solution and the mixture of CMC–AFT was left to stir until the AFT salt is dissolved and become homogenous. The homogenous CMC–AFT solution was then cast into petri dish and put into oven (50 °C) for 12 hours to dry. The AFT composition for each sample was calculated using Eq. (1) where *x* is the weight of AFT salt and *y* is the weight of CMC polymer. The weight of AFT salt for each sample was tabulated in Table 1.

$$\frac{x}{x+y} \times 100 = wt.\% \quad (1)$$

Table 1
The CMC–AFT SBE sample composition

Sample	Weight (g)		Salt wt.%
	CMC	AFT	
AFT00	1.00	0.00	0
AFT05		0.05	5
AFT10		0.11	10
AFT15		0.18	15
AFT20		0.25	20
AFT25		0.33	25
AFT30		0.43	30
AFT35		0.54	35
AFT40		0.67	40
AFT45		0.82	45
AFT50		1.00	50

2.2 SBE Characterization

2.2.1 Ionic conductivity measurement

HIOKI impedance analyzer model IM 3570 was employed to measure the impedance data of the SBE system. Each CMC–AFT SBE sample was cut and put between stainless-steel electrode sample holder for testing. The testing was set to frequency range between 50 Hz to 1 MHz and at elevated temperature range between 303K to 373K. The ionic conductivity of the CMC–AFT SBE was calculated using Eq. (2) where t is the sample thickness, R_b is the bulk resistance of the SBE extracted from the impedance data and A is the contact area between sample and sample holder [14]. The ionic conductivity was further analysed by fitting the conductivity to the Arrhenius relation (Eq. (3)) where the σ_o is the pre-exponential factor, E_a is the activation energy, k_b is the Boltzmann constant and T is the absolute temperature [15].

$$\sigma = \frac{t}{R_b \cdot A} \quad (2)$$

$$\sigma = \sigma_o exp \frac{-E_a}{k_B T} \quad (3)$$

2.2.2 Dielectric calculation

The electrical properties of the SBE were further analysed for its dielectric constant (ε_r), dielectric loss (ε_i), real modulus (M_r) and imaginary modulus (M_i) by using Eq. (4) to Eq. (7) respectively. Z_i and Z_r are the imaginary impedance and real impedance obtained from the impedance spectroscopy measurement. ω is the angular frequency ($2\pi f$) and the C_o is the capacitance in a vacuum which is calculated using the following relation:- $C_o = \varepsilon_o A/t$ where ε_o is the permittivity of free space, A is the contact area and t is sample thickness [16].

$$\varepsilon_r(\omega) = \frac{Z_i}{\omega C_o (Z_r{}^2 + Z_i{}^2)} \quad (4)$$

$$\varepsilon_i(\omega) = \frac{Z_r}{\omega C_o (Z_r{}^2 + Z_i{}^2)} \quad (5)$$

$$M_r(\omega) = \frac{\varepsilon_r}{(\varepsilon_r{}^2 + \varepsilon_i{}^2)} \quad (6)$$

$$M_i(\omega) = \frac{\varepsilon_i}{(\varepsilon_r{}^2 + \varepsilon_i{}^2)} \quad (7)$$

2.2.3 Conduction mechanism modelling

The conduction mechanism was determined by using the Eq. (8) (Jonscher's power law). Resolving the σ_{ac} with Eq. (9) gives the relation as shown in Eq. (10). Here *A* is the temperature dependant parameter (pre-exponential factor), ω is angular frequency, *s* is the power law exponent with a range of 0 < S < 1. The ε_i is the calculated dielectric loss (Eq. (5)) and ε_o is the permittivity of free space (8.85×10^{-12} F/m). Applying the logarithmic rule to Eq. (10) give the equation of straight line (Eq. (11)) [17].

$$\sigma\,(\omega) = \sigma_{dc} + \sigma_{ac} \quad (8)$$

$$\sigma_{ac} = \mathrm{A}\omega^s = \varepsilon_o \varepsilon_i \omega \quad (9)$$

$$\varepsilon_i = \frac{A}{\varepsilon_o}\omega^{s-1} \quad (10)$$

$$\ln \varepsilon_i = \ln \frac{A}{\varepsilon_o} + (s-1)\ln \omega \quad (11)$$

3. Results and Discussions

3.1 Ionic Conductivity Analysis

The calculated ionic conductivity of the CMC–AFT SBE at 303K is shown in Figure 1. From the figure, the ionic conductivity for the undoped SBE is at 1.63×10^{-8} S/cm which is similar to another CMC based electrolyte reported [17,18]. Ionic conductivity increases until sample AFT15 at 2.45×10^{-7} S/cm which is attributed to the increased number of charge carriers (H^+) from the doping process. The ionic conductivity of the SBE gradually declined at higher salt composition and reached 1.95×10^{-7} S/cm for sample AFT30. The decrease in ionic conductivity is believed to be due to the AFT salt forming ion aggregates. These aggregates reduce the effective number of mobile charge carriers for the ionic conduction process. However, ionic conductivity surges to 8.00×10^{-6} S/cm for sample AFT35 and 2.33×10^{-5} S/cm for sample AFT40. The increasing ionic conductivity trends continued until it reached the highest ionic conductivity of 1.47×10^{-4} S/cm for sample AFT50. This conducting behaviour can be explained by using the percolation theory.

This theory deals with the connectivity of random distributed elements where insulating material mixed with conducting material can undergo an insulator-to-conductor transition when certain concentration threshold is reached [19-21]. At this concentration threshold, the conductivity will increase significantly. This significant increase is because the conducting materials form a long continuous network which facilitates fast ionic conduction. Similar observation is seen in this work where ionic conductivity increases from 1.9×10^{-7} S/cm (AFT30) to 8.00×10^{-6} S/cm (AFT35). Hence, 35wt.% of AFT salt is the threshold concentration for the AFT salt to form a continuous network. As a note, higher AFT salt composition (>50%) samples were also prepared. However, the AFT salt formed back on the surface of the dried samples which indicates the CMC polymer cannot solvate the salt anymore. Therefore, it was not selected for further testing.

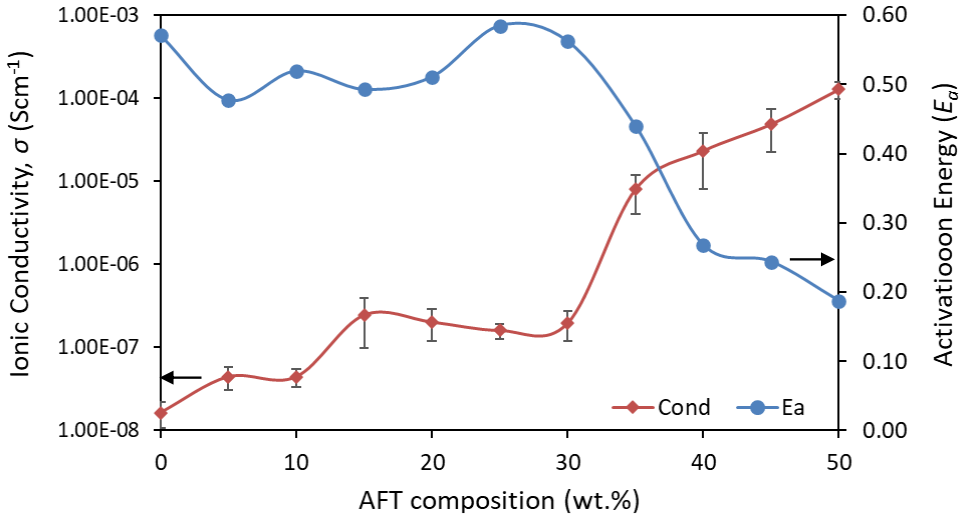

Fig. 1. Ionic conductivity and activation energy value of the CMC–AFT SBE

The ionic conductivity of the SBE at higher temperature is shown in Figure 2. From the figure, the ionic conductivity value increases as the temperature increases. This increase in ionic conductivity is attributed to improved polymer segmental motions and the ease for H^+ dissociations [14,15]. When the temperature increases, the heat energy causes the polymer to vibrate and move the coordinating site closer to the neighbouring chain. This subsequently reduces the energy required for H^+ to initiate conducting process (hopping to coordination site). The activation energy (E_a) of the SBE is calculated from fitting Arrhenius relation (Eq. (3)) with the ionic conductivity and temperature tested. When fitted with the Arrhenius relation, the ionic conductivity trend against temperature shows linear relation where the regression value (R^2) was found to be between 0.97 – 0.99 (Table 2). This proves that the SBE are thermally activated and obey the Arrhenius rule [22].

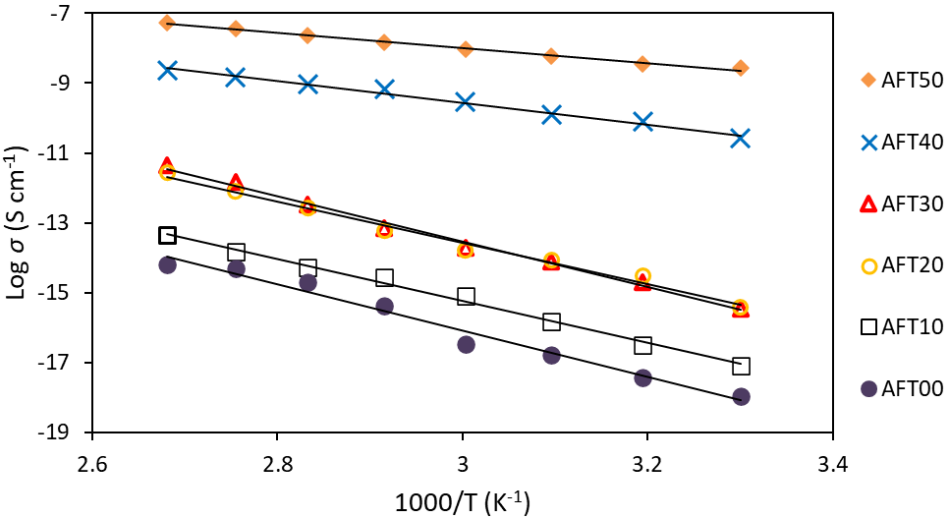

Fig. 2. The ionic conductivity plot of CMC–AFT SBE between 303K to 373K

The E_a of the SBEs was calculated from the gradient of the ionic conductivity plot of the CMC–AFT SBE between 303K to 373K where the value is illustrated in Figure 1 and the tabulated in Table 2. From the table, the E_a value for the CMC–AFT SBE is in inverse trends compared to the ionic conductivity trends where the E_a decreases until AFT15 before it slowly increases until AFT25 and steadily dropped at higher AFT composition. The E_a value dropped until it reached the lowest value at AFT50 which corresponds to the sample with the highest ionic conductivity. This shows the H^+

need lower energy to start the conduction process (releasing and coordinating) thus the high ionic conductivity at AFT50.

Table 2
The ionic conductivity value of the CMC–AFT SBE sample with the regression value (R^2) and activation energy (E_a) of the sample

Sample	Ionic conductivity, σ (S/cm)		Regression	Activation energy,
	303K	373K	R^2	E_a (eV)
AFT00	1.63×10^{-8}	6.72×10^{-7}	0.977	0.571
AFT05	4.42×10^{-8}	9.86×10^{-7}	0.985	0.477
AFT10	4.74×10^{-8}	1.57×10^{-6}	0.993	0.519
AFT15	2.45×10^{-7}	6.84×10^{-6}	0.991	0.493
AFT20	2.02×10^{-7}	9.55×10^{-6}	0.989	0.511
AFT25	1.60×10^{-7}	8.42×10^{-6}	0.991	0.585
AFT30	1.95×10^{-7}	1.19×10^{-5}	0.993	0.563
AFT35	8.00×10^{-6}	2.45×10^{-5}	0.989	0.440
AFT40	2.33×10^{-5}	1.77×10^{-4}	0.988	0.268
AFT45	4.87×10^{-5}	2.47×10^{-4}	0.972	0.244
AFT50	1.47×10^{-4}	7.02×10^{-4}	0.983	0.187

3.2 Dielectric Analysis

Dielectric constant, ε_r property in SBE indicates the stored charge capacity of the SBE when polarized by electric field thus further verify the ionic conductivity behaviour [23,24]. The dielectric properties of the SBE were calculated using Eq. (4) to Eq. (7). Figure 3 shows the ε_r value at selected frequency (1KHz) for each CMC–AFT SBE samples at 303K. The value shows trends similar to the ionic conductivity value where the value increases to AFT15 then slightly reduces until AFT before they further increase back at AFT35 until AFT50. The increase dielectric value is due to the low lattice energy of AFT salt (~737 KJ/mol) which allow for H^+ to dissociate from ammonium salt when induced by electric field thus increasing SBE's ability to store charges as AFT salt increases [25].

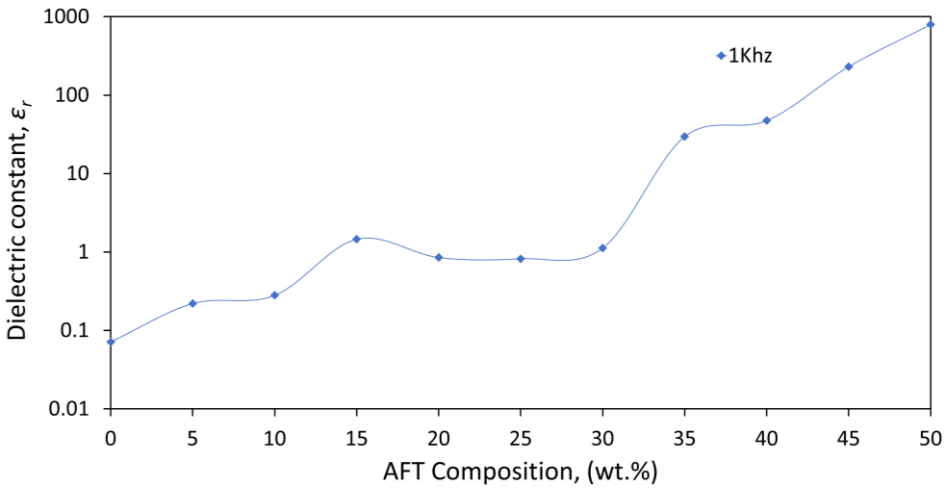

Fig. 3. The Dielectric constant value of CMC–AFT SBE at selected frequency

Figure 4 shows the dielectric constant (ε_r) plot for selected CMC–AFT SBE samples (AFT00, AFT10, AFT20, AFT30, AFT40, AFT50) at higher temperature (303K – 373K) and at frequency range of 50 Hz to 1MHz. Similar trends for all CMC–AFT SBE samples can be seen where the ε_r value is higher at the low frequency region. The value then gradually declines as frequency increases and becomes

saturated at very high frequency region. The high ε_r value at low frequency indicates that the SBE is capable of polarizing along the electric field direction especially for the samples at higher AFT composition. This is due to the AFT low lattice energy, making it more susceptible for H^+ dissociation with the electric field. At higher frequencies, the electric field direction changes at higher rate which causes the H^+ lagging to diffuse towards the electric field direction [16]. This reduces the time for H^+ to be polarize, resulting in reduced dielectric value. At the very high frequency ($4 \geq \omega \geq 6$), the H^+ are stuck within their potential well thus impedes their polarization, which resulted in the flat dielectric value shown in the figure.

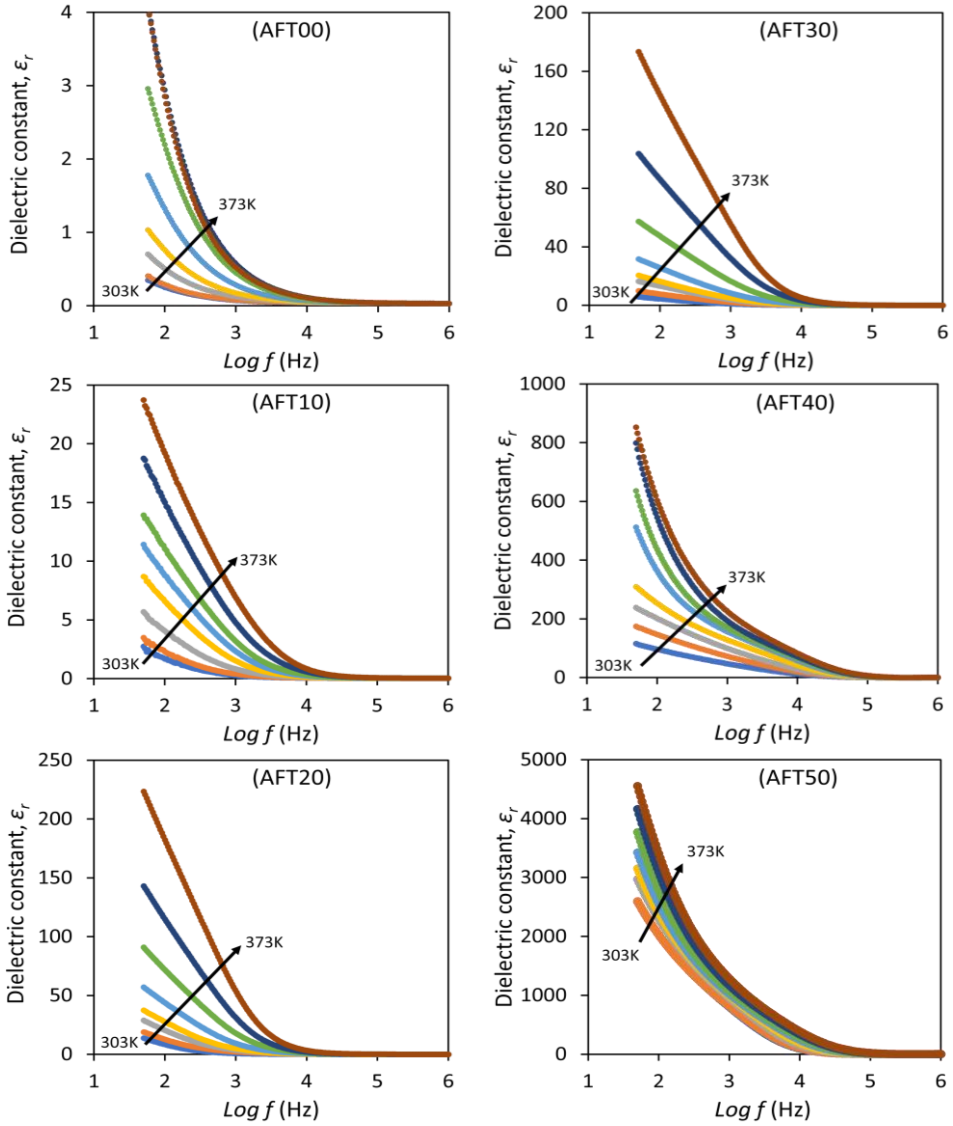

Fig. 4. Dielectric constant for selected CMC–AFT SBE at higher temperature

The increase in ε_r value with temperature for all CMC–AFT SBE samples can be explained by two factors. The first is due to the increased dissociation of H^+ from AFT salt due to increase in heat energy. The second factor is the increased polymer segmental motion which improved the H^+ migrations. At higher temperature, similar behaviour was seen for all SBE samples across the tested frequency where the ε_r value is higher at low frequency region and gradually decreases. However, the increased AFT salt dissociation and segmental motion still unable to follow the fast electric field changes at high frequency regions ($4 \geq \omega \geq 6$), thus the flat dielectric value seen in the figure.

The dielectric was further analysed for the dielectric modulus. The dielectric modulus corresponds to the physical relaxation process in the SBE by eliminating the electrode polarization and other interfacial effects [26-28]. The plot of imaginary modulus for selected CMC–AFT SBE samples (AFT00, AFT10, AFT20, AFT30, AFT40, AFT50) at 303K temperature are shown in Figure 5. Clear relaxation peaks (single peak) within the tested frequency range can be seen for sample AFT00, AFT10, AFT20 and AFT30. The relaxation peaks indicate the H^+ ability to move within the SBE. The region between the low frequency to the relaxation peak (M_{max}) shows the mobile H^+ ability to migrate on long distances while the region from the M_{max} to the highest frequency shows the H^+ mobility is on short distances due to being confined to their potential wells [29]. The relaxation peak can be seen to shift to higher frequency as the AFT salt increases. The shift is due to the AFT salt dissociation into free H^+ and migrate with the electric field, hence the relaxation peak shift. No relaxation peak was observed for AFT40 and AFT50, instead both sample shows a very low M_i value and slightly increases at the very high frequency. No relaxation peak observed is believed due to the limitation of frequency tested (f_{max} = 1 MHz).

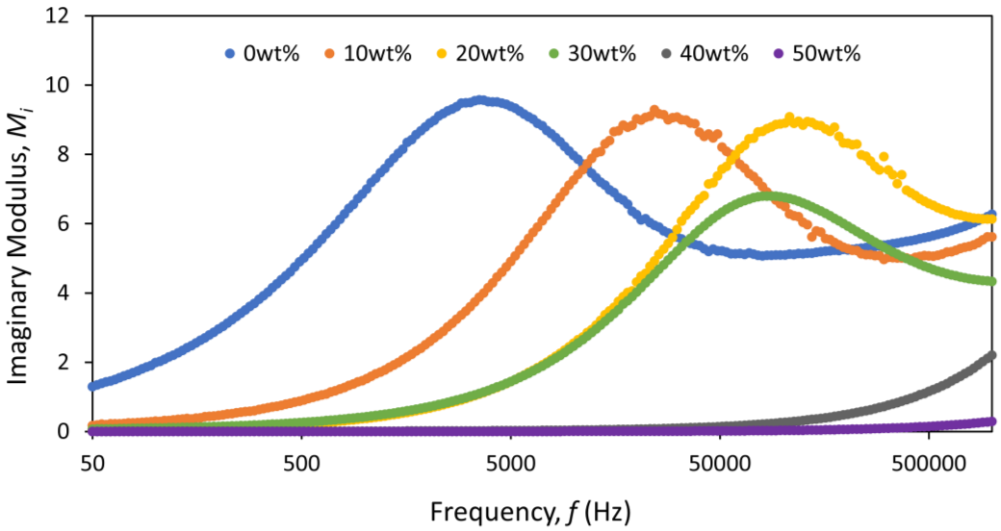

Fig. 5. Dielectric modulus for selected CMC–AFT SBE at 303K temperature

Figure 6 shows the dielectric modulus for selected CMC–AFT SBE (AFT00, AFT10, AFT20, AFT30, AFT40, AFT50) at higher temperature. The relaxation peak shown to shift to higher frequencies as temperature increased. When the temperature increases, the H^+ movement improves (faster) due to the excessive energy absorbed (temperature). The H^+ can hop to the adjacent coordination site when induced by the electric field. This allows for H^+ to move farther with the electric field orientation thus the ionic conductivity of the SBE rises at higher temperature. The observed peak also appears to be asymmetrical to the centre of the peak (M_{max}). This shows that the CMC–AFT SBE follows non-Debye relaxation behaviour where different relaxation processes occurred within the SBE which could be associated to the AFT salt aggregation and polymer chain motion [30]. Relaxation peak is not present for AFT40 and AFT50 sample as temperature increases due to the limitation of frequencies tested. However, the M_i value appears to shift to a higher frequency with increasing temperature which means that H^+ could migrate farther within the SBE.

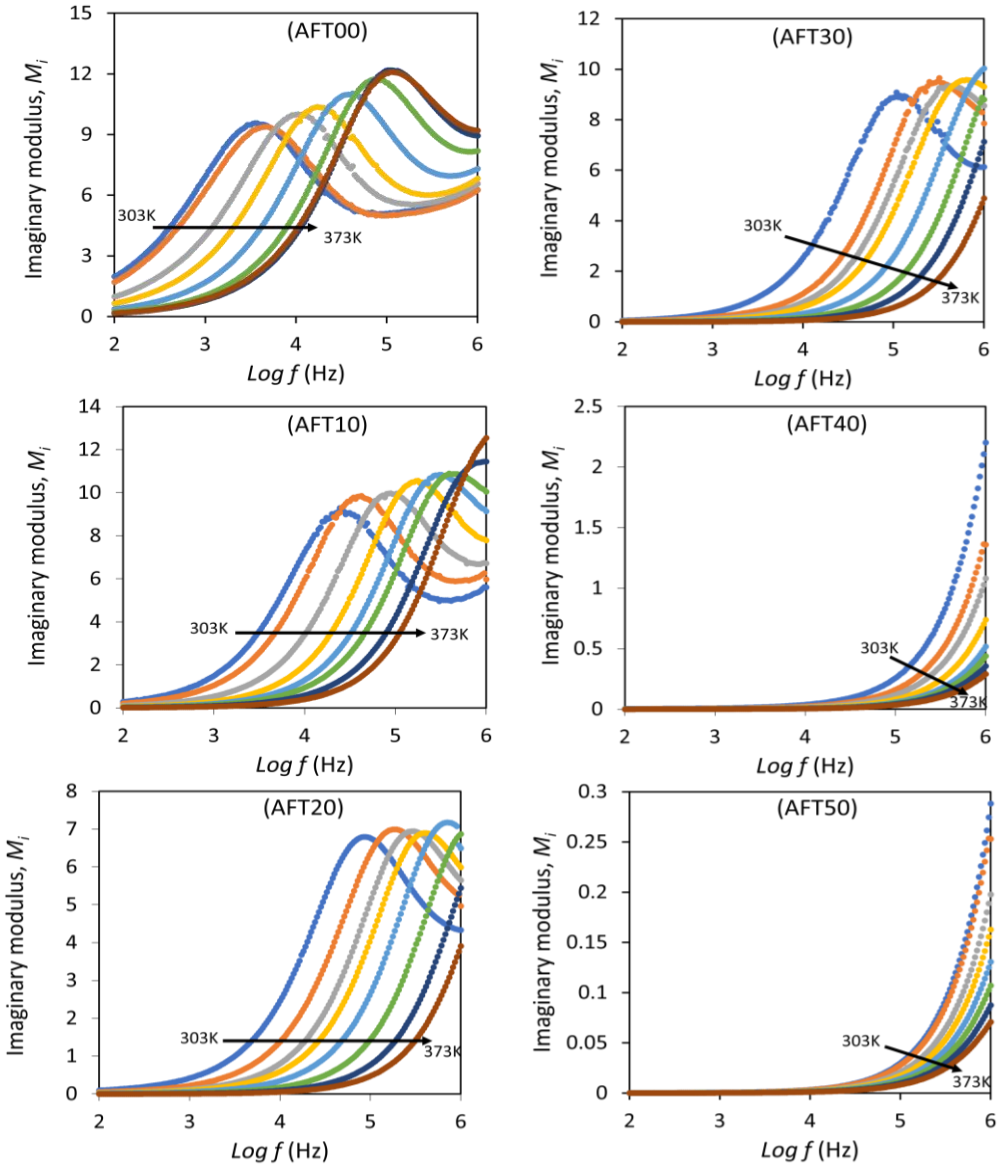

Fig. 6. Imaginary modulus for selected CMC–AFT SBE at higher temperature

3.3 Conduction Mechanism

The mechanism in which the H^+ moved in the SBE was analysed using Jonscher's universal power law relationship (Eq. (8) to Eq. (11)) and fitted to different conduction mechanism model namely as correlated barrier hopping (CBH), quantum mechanical tunnelling (QMT), overlapping large polaron tunnelling (OLPT) and non-overlapping small polaron tunnelling (NSPT) [31,32]. The *S* value represents the degree of interaction between mobile ions with the surrounding lattices [33].

The *S* value against temperature (*T*) was extracted from the gradient of ln ε_i with ln ω plot (Figure 7(a)) at high frequency region ($12 \leq \ln \omega \leq 14$) to remove the effect of space charge polarization. The variation of *S* with *T* is plotted in Figure 7(b). Based on the figure, the value of *S* shows miniscule variations within the temperature range (303K – 373K) resulting in a very low gradient value (-0.0003x + 0.2771) and can be assumed to be temperature independent. Therefore, the conduction mechanism for the AFT50 can be explained by the QMT model. In this model, polarons (made up of H^+ and the stress field) can tunnel through the potential barrier between the coordination sites which are usually forbidden in the classical model for conduction process. The tunnelling process explained

how ionic conductivity increases at higher AFT salt composition and the low activation energy, E_a. Similar conduction mechanism was also attained in the CMC-Ammonium nitrate SBE system reported previously [17].

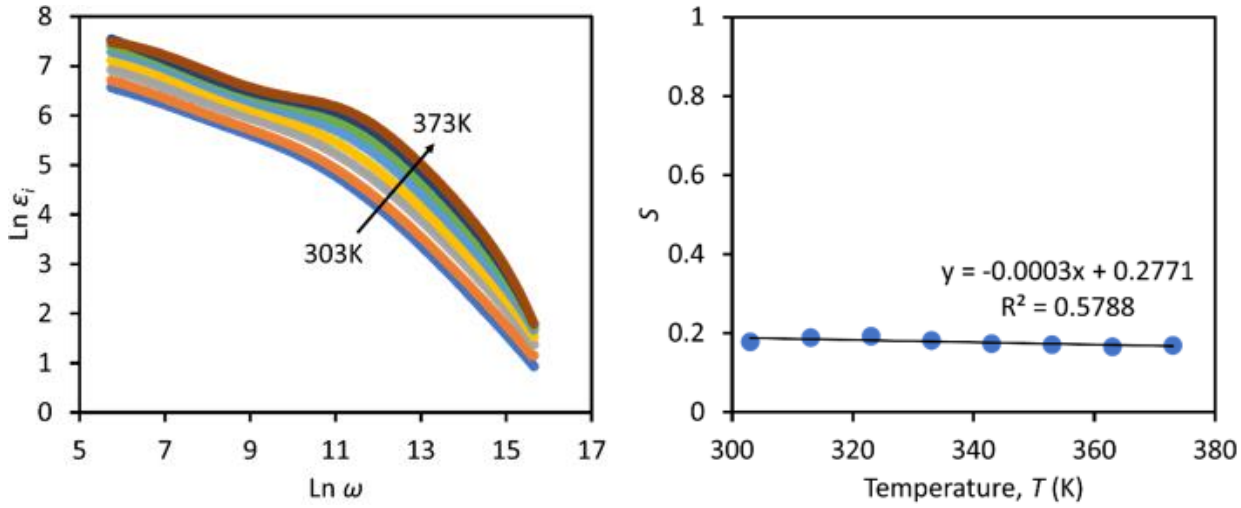

(a) (b)

Fig. 7. (a) The plot of ln ε_i against ln ω to extract S value. (b) the variation value of S at different temperatures, T

4. Conclusions

The CMC based SBE ionic conductivity and electrical properties has clearly improved from the doping of ammonium formate salt. The highest ionic conductivity of the CMC–AFT SBE achieved is 1.47×10^{-4} S/cm and is thermally stable up until 373K. The CMC-AFT SBE also follows the Arrhenius behaviour (R^2~1). The ionic conductivity trends shows that percolation network existed at higher salt composition and is supported from the disappearance of relaxation mechanism in dielectric analysis. The low E_a value coupled with the QMT model supports the percolation behaviour observed in the SBE system. Therefore, the effect of percolation should be considered before deciding the range of salt composition for a new polymer electrolyte system with the highest ionic conductivity. The highest ionic conductivity achieved was just above $\times 10^{-4}$ S/cm, so it is not suitable for electrochemical application. Therefore, the SBE needs to be improved further before the SBE can be applied and tested in electrochemical application. The incorporation of plasticizer or oxide-based filler can further improve the ionic conductivity of the CMC-AFT SBE.

Acknowledgement

This research was funded by a grant from Universiti Sains Islam Malaysia (USIM – 19123).

References

[1] Ponrouch, Alexandre, Jan Bitenc, Robert Dominko, Niklas Lindahl, Patrik Johansson, and M. Rosa Palacín. "Multivalent rechargeable batteries." *Energy Storage Materials* 20 (2019): 253-262. https://doi.org/10.1016/j.ensm.2019.04.012

[2] Chen, Yuqing, Yuqiong Kang, Yun Zhao, Li Wang, Jilei Liu, Yanxi Li, Zheng Liang et al. "A review of lithium-ion battery safety concerns: The issues, strategies, and testing standards." *Journal of Energy Chemistry* 59 (2021): 83-99. https://doi.org/10.1016/j.jechem.2020.10.017

[3] Wu, Chaoshan, Jiatao Lou, Jun Zhang, Zhaoyang Chen, Akshay Kakar, Benjamin Emley, Qing Ai et al. "Current status and future directions of all-solid-state batteries with lithium metal anodes, sulfide electrolytes, and layered transition metal oxide cathodes." *Nano Energy* 87 (2021): 106081. https://doi.org/10.1016/j.nanoen.2021.106081

[4] Maia, Beatriz Arouca, Natália Magalhães, Eunice Cunha, Maria Helena Braga, Raquel M. Santos, and Nuno Correia. "Designing versatile polymers for lithium-ion battery applications: a review." *Polymers* 14, no. 3 (2022): 403. https://doi.org/10.3390/polym14030403

[5] Udayakumar, Gowthama Prabu, Subbulakshmi Muthusamy, Bharathi Selvaganesh, N. Sivarajasekar, Krishnamoorthy Rambabu, Fawzi Banat, Selvaraju Sivamani, Nallusamy Sivakumar, Ahmad Hosseini-Bandegharaei, and Pau Loke Show. "Biopolymers and composites: Properties, characterization and their applications in food, medical and pharmaceutical industries." *Journal of Environmental Chemical Engineering* 9, no. 4 (2021): 105322. https://doi.org/10.1016/j.jece.2021.105322

[6] Gupta, Shikha, and Pradeep K. Varshney. "Effect of plasticizer on the conductivity of carboxymethyl cellulose-based solid polymer electrolyte." *Polymer Bulletin* 76, no. 12 (2019): 6169-6178. https://doi.org/10.1007/s00289-019-02714-1

[7] Dueramae, Isala, Manunya Okhawilai, Pornnapa Kasemsiri, Hiroshi Uyama, and Rio Kita. "Properties enhancement of carboxymethyl cellulose with thermo-responsive polymer as solid polymer electrolyte for zinc ion battery." *Scientific Reports* 10, no. 1 (2020): 12587. https://doi.org/10.1038/s41598-020-69521-x

[8] Cyriac, Vipin, Ismayil, I. M. Noor, Kuldeep Mishra, Chetan Chavan, Rajashekhar F. Bhajantri, and Saraswati P. Masti. "Ionic conductivity enhancement of PVA: carboxymethyl cellulose poly-blend electrolyte films through the doping of NaI salt." *Cellulose* 29, no. 6 (2022): 3271-3291. https://doi.org/10.1007/s10570-022-04483-z

[9] Meng, Yating, Chuanhao Nie, Weijia Guo, Deng Liu, Yaxin Chen, Zhicheng Ju, and Quanchao Zhuang. "Inorganic cathode materials for potassium ion batteries." *Materials Today Energy* 25 (2022): 100982. https://doi.org/10.1016/j.mtener.2022.100982

[10] Khan, Nadeem, Guihong Han, and Shaukat Ali Mazari. "Carbon nanotubes-based anode materials for potassium ion batteries: A review." *Journal of Electroanalytical Chemistry* 907 (2022): 116051. https://doi.org/10.1016/j.jelechem.2022.116051

[11] Xia, Fanjie, Haoyang Peng, Qi Liang, Xin Peng, Congli Sun, and Jinsong Wu. "Serial cracking in Van der Waals layered electrodes mediated by electrochemical reaction and mechanical deformation." *Cell Reports Physical Science* 2, no. 11 (2021): 100642. https://doi.org/10.1016/j.xcrp.2021.100642

[12] Guo, Haocheng, Damian Goonetilleke, Neeraj Sharma, Wenhao Ren, Zhen Su, Aditya Rawal, and Chuan Zhao. "Two-Phase Electrochemical Proton Transport and Storage in α-MoO3 for Proton Batteries." *Cell Reports Physical Science* 1, no. 10 (2020): 100225. https://doi.org/10.1016/j.xcrp.2020.100225

[13] Hadi, Jihad M., Shujahadeen B. Aziz, Hwda Ghafur Rauf, Rebar T. Abdulwahid, Sameerah I. Al-Saeedi, Dana A. Tahir, and Mohd Fakhrul Zamani Kadir. "Proton conducting polymer blend electrolytes based on MC: FTIR, ion transport and electrochemical studies." *Arabian Journal of Chemistry* 15, no. 11 (2022): 104172. https://doi.org/10.1016/j.arabjc.2022.104172

[14] Balakrishnan, N. T. M., A. Das, J. D. Joyner, MJ Jabeen Fatima, L. R. Raphael, A. Pullanchiyodan, and P. Raghavan. "Quest for high-performance gel polymer electrolyte by enhancing the miscibility of the bi-polymer blend for lithium-ion batteries: performance evaluation in extreme temperatures." *Materials Today Chemistry* 29 (2023): 101407. https://doi.org/10.1016/j.mtchem.2023.101407

[15] Banitaba, Seyedeh Nooshin, Dariush Semnani, Elahe Heydari-Soureshjani, Behzad Rezaei, and Ali A. Ensafi. "The effect of concentration and ratio of ethylene carbonate and propylene carbonate plasticizers on characteristics of the electrospun PEO-based electrolytes applicable in lithium-ion batteries." *Solid State Ionics* 347 (2020): 115252. https://doi.org/10.1016/j.ssi.2020.115252

[16] Naiwi, Tuan Syarifah Rossyidah Tuan, Min Min Aung, Marwah Rayung, Azizan Ahmad, Kai Ling Chai, Mark Lee Wun Fui, Emma Ziezie Mohd Tarmizi, and Nor Azah Abdul Aziz. "Dielectric and ionic transport properties of bio-based polyurethane acrylate solid polymer electrolyte for application in electrochemical devices." *Polymer Testing* 106 (2022): 107459. https://doi.org/10.1016/j.polymertesting.2021.107459

[17] Kamarudin, Khadijah Hilmun, and Mohd Ikmar Nizam Mohamad Isa. "Ionic conductivity via quantum mechanical tunneling in NH_4NO_3 doped carboxymethyl cellulose solid biopolymer electrolytes." *Advanced Materials Research* 1107 (2015): 236-241. https://doi.org/10.4028/www.scientific.net/AMR.1107.236

[18] Sohaimy, M. I. H., and M. I. N. Isa. "Ionic conductivity and conduction mechanism studies on cellulose based solid polymer electrolytes doped with ammonium carbonate." *Polymer Bulletin* 74 (2017): 1371-1386. https://doi.org/10.1007/s00289-016-1781-5

[19] Urban, Alexander. "Modeling ionic transport and disorder in crystalline electrodes using percolation theory." In *Computational Design of Battery Materials*, pp. 169-185. Cham: Springer International Publishing, 2024. https://doi.org/10.1007/978-3-031-47303-6_6

[20] Ponnamma, Deepalekshmi, Neethu Ninan, and Sabu Thomas. "Carbon nanotube tube filled polymer nanocomposites and their applications in tissue engineering." In *Applications of Nanomaterials*, pp. 391-414. Woodhead Publishing, 2018. https://doi.org/10.1016/B978-0-08-101971-9.00014-4

[21] Hajar, M. D. Siti, A. G. Supri, and A. J. Jalilah. "The Effect of Poly (ethylene glycol) Diglycidyl Ether as Surface Modifier on Conductivity and Morphology of Carbon Black-Filled Poly (vinyl chloride)/Poly (ethylene oxide) Conductive Polymer Films." *Journal of Advanced Research Design* 10, no. 1 (2015): 9-13.

[22] Zheng, Jinyun, Jiawei Zhang, Wenjie Li, Junmin Ge, and Weihua Chen. "Phosphate-based gel polymer electrolyte enabling remarkably long cycling stable sodium storage in a wide-operating-temperature." *Chemical Engineering Journal* 465 (2023): 142796. https://doi.org/10.1016/j.cej.2023.142796

[23] Arya, Anil, and A. L. Sharma. "Tailoring of the structural, morphological, electrochemical, and dielectric properties of solid polymer electrolyte." *Ionics* 25 (2019): 1617-1632. https://doi.org/10.1007/s11581-019-02916-7

[24] Abdulkadir, Bashir Abubakar, John Ojur Dennis, Muhammad Fadhlullah Bin Abd Shukur, Mohamed Mahmoud Elsayed Nasef, and Fahad Usman. "Study on dielectric properties of gel polymer electrolyte based on PVA-K_2Co3 composites." *International Journal of Electrochemical Science* 16, no. 1 (2021): 150296. https://doi.org/10.20964/2021.01.34

[25] Sohaimy, M. I. H., and M. I. N. Isa. "Proton-conducting biopolymer electrolytes based on carboxymethyl cellulose doped with ammonium formate." *Polymers* 14, no. 15 (2022): 3019. https://doi.org/10.3390/polym14153019

[26] Mtioui, O., H. Litaiem, Santiago Garcia-Granda, L. Ktari, and Mohamed Dammak. "Thermal behavior and dielectric and vibrational studies of $Cs_2(HAsO_4)_{0.32}(SO_4)_{0.68}{\cdot}Te(OH)_6$." *Ionics* 21 (2015): 411-420. https://doi.org/10.1007/s11581-014-1196-y

[27] Coşkun, Merve, Özgür Polat, Fatih Mehmet Coşkun, Zehra Durmuş, Müjdat Çağlar, and Abdulmecit Türüt. "The electrical modulus and other dielectric properties by the impedance spectroscopy of $LaCrO_3$ and $LaCr0.90Ir0.10O_3$ Perovskites." *RSC Advances* 8, no. 9 (2018): 4634-4648. https://doi.org/10.1039/C7RA13261A

[28] Chérif, Saïda Fatma, Amira Chérif, Wassim Dridi, and Mohamed Faouzi Zid. "Ac conductivity, electric modulus analysis, dielectric behavior and Bond Valence Sum analysis of $Na_3Nb_4As_3O_{19}$ compound." *Arabian Journal of Chemistry* 13, no. 6 (2020): 5627-5638. https://doi.org/10.1016/j.arabjc.2020.04.003

[29] Dam, Tapabrata, Sidhartha S. Jena, and Dillip K. Pradhan. "Coupled ion conduction mechanism and dielectric relaxation phenomenon in PEO_{20}-$LiCF_3SO_3$-based ion conducting polymer nanocomposite electrolytes." *The Journal of Physical Chemistry C* 122, no. 8 (2018): 4133-4143. https://doi.org/10.1021/acs.jpcc.7b11112

[30] Tang, Rujun, Chen Jiang, Wenhu Qian, Jie Jian, Xin Zhang, Haiyan Wang, and Hao Yang. "Dielectric relaxation, resonance and scaling behaviors in $Sr_3Co_2Fe_{24}O_{41}$ hexaferrite." *Scientific Reports* 5, no. 1 (2015): 13645. https://doi.org/10.1038/srep13645

[31] Radoń, Adrian, Dariusz Łukowiec, Marek Kremzer, Jarosław Mikuła, and Patryk Włodarczyk. "Electrical conduction mechanism and dielectric properties of spherical shaped Fe_3O_4 nanoparticles synthesized by co-precipitation method." *Materials* 11, no. 5 (2018): 735. https://doi.org/10.3390/ma11050735

[32] Dhaou, Mohamed Houcine, Abdulrahman Mallah, and Abdulrahman Alsawi. "Dielectric Relaxation and Non-Overlapping Small Polaron Tunneling Model Conduction Studies of $Ag_{2-x}Na_xZnP_2O_7$ (x= 0, 1, and 2) Materials." *Crystal Research and Technology* 56, no. 9 (2021): 2100035. https://doi.org/10.1002/crat.202100035

[33] Mostafa, Mohga F., and Ahmed K. Tammam. "Overlap large polaron sensitivity to phase changes in the first alkali earth organic-inorganic hybrid:$[(CH_2)_7(NH_3)_2]CaCl_4$." *Journal of Physics and Chemistry of Solids* 161 (2022): 110376. https://doi.org/10.1016/j.jpcs.2021.110376